Biomaterials Science

ROYAL SOCIETY OF CHEMISTRY

PAPER

View Article Online
View Journal | View Issue

Open Access Article. Published on 24 June 2020. Downloaded on 10/19/2025 9:03:45 PM.
This article is licensed under a Creative Commons Attribution 3.0 Unported Licence.

Check for updates

Cite this: *Biomater. Sci.*, 2020, **8**, 4239

Tough and injectable fiber reinforced calcium phosphate cement as an alternative to polymethylmethacrylate cement for vertebral augmentation: a biomechanical study†

Sónia de Lacerda Schickert, João Castro Pinto, John Jansen, Sander C. G. Leeuwenburgh and Jeroen J. J. P. van den Beucken *

Received 13th March 2020,
Accepted 15th June 2020

DOI: 10.1039/d0bm00413h

rsc.li/biomaterials-science

Vertebral compression fractures (VCFs) are a very common problem among the elderly, which ultimately result in severe pain and a drastically reduced quality of life. An effective treatment for VCFs is the minimally invasive augmentation of the damaged vertebrae through vertebroplasty and/or kyphoplasty. These surgical procedures treat the affected vertebrae by injection of poly(methyl methacrylate) cement (PMMA) into the vertebral body. However, clinical use of PMMA cement is associated with major drawbacks. Bioceramic cements such as injectable calcium phosphate cements (CPC) exhibit a superior osteocompatibility over PMMA cements, but are too brittle for load-bearing applications. Here, we evaluated the handling and mechanical properties of a recently developed CPC formulation containing both poly(vinyl alcohol) (PVA) fibers and carboxymethyl cellulose (CMC) as an alternative to PMMA cement for vertebro- and kyphoplasty. Our results demonstrate that the addition of CMC rendered fiber-reinforced CPC injectable without negatively affecting its mechanical properties. Further, an *ex vivo* mechanical analysis clearly showed that extravasation of PVA fiber-reinforced CPC with CMC into trabecular bone was limited as compared to PMMA. Finally, we observed that the *ex vivo* biomechanical performance of vertebrae treated with CMC and PVA fibers was similar to PMMA-treated vertebrae. The obtained data suggests that PVA fiber-reinforced CPCs with CMC possesses adequate handling, mechanical and structural characteristics for vertebro- and kyphoplasty procedures. These data pave the way for future preclinical studies on the feasibility of treating vertebral compression fractures using PVA fiber-reinforced CPC with CMC.

1. Introduction

Over the past decades, population aging has become a global trend. United Nations estimate that 16% of the world population will be 65 years or older by 2050.[1] As a consequence, age-related diseases such as osteoporosis have increased the prevalence of vertebral compression fractures (VCFs), which have evolved into a major global social and economic burden.[2] VCFs are the most common type of bone fracture among elderly diagnosed with osteoporosis, showing an incidence of 20% among the elderly population.[2,3] These fractures frequently result in both acute and chronic pain, leading to dramatic physical, functional and psychological impairment and ultimately increased morbidity and even mortality.[2–4]

Vertebral augmentation procedures such as vertebroplasty and kyphoplasty have been suggested as an effective treatment for VCFs.[2,3,5–7] Both procedures involve a minimally invasive surgical procedure for the transpedicular delivery of poly (methyl methacrylate) (PMMA) cement into the vertebral body.[3,4,6,8] While vertebroplasty includes the injection of cement directly into the vertebra, kyphoplasty uses an inflatable bone tamp placed within the cancellous portion of the vertebral body, that once inflated creates a bone cavity that is subsequently filled with PMMA.[2,4,5] These procedures successfully stabilize VCFs, relieve the pain immediately after the surgery, and allow patients to rapidly resume their daily activities.

In vertebro- and kyphoplasty procedures, PMMA is the preferred filling material since this polymer is bioinert, easy to handle, cost-efficient and mechanically strong.[2,9] In addition, radiopacifiers such as barium sulphate have been added to PMMA to render the cement radiopaque and allow for monitoring its correct injection within the vertebral body during the surgical procedure.[2,4] Despite the clinical success of PMMA for

Radboud University Medical Center, Radboud Institute for Molecular Life Sciences; Department of Dentistry - Regenerative Biomaterials, Philips van Leydenlaan 25, Nijmegen, The Netherlands. E-mail: Jeroen.vandenBeucken@radboudumc.nl

† Electronic supplementary information (ESI) available. See DOI: 10.1039/d0bm00413h

Open Access Article. Published on 24 June 2020. Downloaded on 10/19/2025 9:03:45 PM.
This article is licensed under a Creative Commons Attribution 3.0 Unported Licence.

these applications, several complications are associated with the intra-operative and long-term application of PMMA. Intra-operatively, the high exothermic polymerization temperature (*i.e.* >70 °C) of PMMA causes thermal necrosis of the tissue surrounding the injection site, while its high flowability can lead to material leakage. Indeed, the incidence of PMMA leakage is reported to be 41%–59.7% in vertebroplasty and 9%–18.4% in kyphoplasty.[10,11] Cement leakage can cause compression and damage of the spinal cord when PMMA leaks into the spinal cord or pulmonary embolism if the material leaks into the surrounding blood vessels.[2,5] Moreover, incomplete PMMA polymerization leads to release of cytotoxic PMMA monomers, which causes local inhibition of bone perfusion and bone resorption.[12] Finally, a serious mismatch exists between the mechanical properties of PMMA and the bone tissue in vertebral bodies, as demonstrated by PMMA stiffness values which are 7–10 fold higher than cancellous bone.[9] Multiple studies have shown that vertebrae adjacent to PMMA-treated vertebral bodies are up to 3 times more likely to fail than those further away.[6,13] These findings support the theory that the use of traditional PMMA in vertebro- and kyphoplasty negatively impacts spine biomechanics.[6,7,13,14]

Calcium phosphate cements (CPCs) are already used as alternative to PMMA cement in vertebral augmentation procedures performed in less challenging scenarios (*e.g.* young patients).[12,15] Apatitic CPCs represent a unique class of bioceramics characterized by (i) a chemical composition similar to the hydroxyapatite phase present in native bone, (ii) a highly osteocompatible tissue response, and (iii) the capability to form a direct bond with bone.[16–19] CPCs are composed of a powder phase (composed by one of more orthophosphate powders), that form an injectable paste able to set and harden under physiological conditions when mixed with a liquid phase (*e.g.* water or an aqueous solution). Moreover, and contrarily to the exothermic polymerization occurring in PMMA, CPCs set as a result of dissolution and reprecipitation reactions that are almost isothermal.[19,20] Nevertheless, CPCs are still associated with two major drawbacks that severely limit their applicability: (i) poor cohesion and washout resistance and (ii) sub-optimal mechanical properties.

The poor cohesion of CPCs causes (partial) disintegration shortly after injection *in situ*, upon early contact with blood or other fluids.[21] Specifically for highly perfused vertebral applications, cement disintegration may cause leakage of CPC particles into the blood stream, which can lead to systemic complications (*e.g.* blood clotting and pulmonary embolism).[2,22] Interestingly, the lubricant carboxymethyl cellulose (CMC) has the capacity to improve both cohesion and wash-out profiles of CPC pastes;[22–25] additionally, the long-term *in vivo* biocompatibility of CPC/CMC pastes has been previously confirmed.[24] Moreover, in an attempt to overcome the intrinsic brittleness and limited toughness of CPCs,[12,17,19,20] we recently developed a novel poly(vinyl alcohol) (PVA) fiber-reinforced CPC (frCPC), with confirmed cytocompatibility of the selected PVA fibers[26] and enhanced mechanical strength and fracture toughness without compromising osteocompatibility.[26,27] Furthermore, the wettability of PVA fibers, and its influence on the fiber-matrix interfacial shear strength has also been characterized.[28] Although promising, the previously developed frCPCs still have suboptimal handling properties (*i.e.* frCPCs are only moldable), hindering the application of these materials through minimally invasive injection performed during vertebro- and kyphoplasty procedures.

Therefore, we here developed and optimized for the first time an injectable form of PVA-reinforced CPC and further analyzed its suitability for vertebral augmentation procedures. For this purpose, we comparatively evaluated the material properties of frCPCs and PMMA using a range of *in vitro* and *ex vivo* techniques that aimed to mimic vertebral augmentation procedures as close as possible. Accordingly, (i) injectability was measured using a clinically available cannula developed specifically for vertebral augmentation, (ii) setting time and cohesion were assessed considering vertebral augmentation standards, (iii) frCPCs and PMMA were subjected to loads typically found in the vertebral column and (iv) vertebrae were selected for the *ex vivo* biomechanical test. We hypothesized that the addition of CMC to frCPC would improve the handling properties for injectable applications, while reinforcement with PVA fibers would increase their mechanical performance.

2. Experimental

2.1. Preparation of the injectable frCPC

The solid phase of the frCPC was composed of α-tricalcium phosphate (α-TCP, Cam Bioceramics B.V., Leiden, The Netherlands), sodium carboxymethyl cellulose (CMC, kindly provided by Barentz International B.V., Hoofddorp, The Netherlands) and poly(vinyl alcohol) fibers (PVA, MiniFIBERS Inc., Johnson City, TN, USA) at different concentrations, according to Table 1. The α-TCP powder consisted of 100% pure, milled α-TCP microparticles, with a mean particle size of ~4.0 μm. The selected CMC powder was a pharmaceutical grade sodium CMC (degree of substitution: 0.86, Blanose 9H4XF-PH) which was sieved to remove particles larger than 106 μm. Finally, the selected PVA fibers (length: 1500 μm; diameter: 14 μm) were hand-cut in bundles by using a precision-scalpel (blade no. 11, W.R. Swann & Co. Ltd, Sheffield, USA) and further separated from each other by sieving. All solid components were homogeneously mixed with the liquid phase, a 4 wt% $NaH_2PO_4 \cdot 2H_20$ (Merck, Darmstadt, Germany) aqueous solution, at a 1 : 2 liquid-to-powder ratio.

Table 1 Composition of the solid phase of the experimental groups

Experimental groups	CPC [wt%]	CMC [wt%]	PVA [wt%]
CPC	100.0	—	—
$frCPC_{2\%}$	98.0	—	2.0
$frCPC_{3\%}$	97.0	—	3.0
CPC/CMC	98.5	1.5	—
$frCPC/CMC_{2\%}$	96.5	1.5	2.0
$frCPC/CMC_{3\%}$	95.5	1.5	3.0

 This journal is © The Royal Society of Chemistry 2020

Open Access Article. Published on 24 June 2020. Downloaded on 10/19/2025 9:03:45 PM.
This article is licensed under a Creative Commons Attribution 3.0 Unported Licence.

2.2. Assessment of handling properties: setting time, injectability and cohesion analysis

Initial and final setting times of the frCPC compositions were studied by using a standardized Gillmore needle protocol, adapted from ASTM C266-89. In brief, frCPCs were mixed and inserted into a bronze mold (diameter: 6 mm; height: 12 mm), previously placed in a 37 °C water heated bath. Light- and heavy-weighted needles were then used to determine initial and final setting time. Setting time was recorded from the moment the liquid phase was added to the solid phase until the timepoint where indentation in the cement surface was not formed anymore by the light- (initial setting) or heavy-weighted (final setting) needles.

The injectability of CPCs was previously defined as the ability of a paste to remain homogeneous under pressure, during manual extrusion, independent of a defined injection force.[22,23,29] For the current study, the injectability of frCPCs was studied according to a slight adaptation of a previously reported method.[23] In brief, a 3 ml syringe (Luer lock system, Terumo Europe NV, Leuven, Belgium) was coupled to a clinically available coaxial 11G cannula developed specifically for vertebral augmentation (VertePort® Cement Cannula 11G, length: 12.7 cm, Stryker Corporation, Kalamazoo, Michigan, USA) and further used as an extrusion device to mimic vertebral augmentation procedures. The cement was manually mixed with the aid of a spatula and thereafter transferred to the syringe and extruded through the cannula. Care was taken to ensure that the time frame between frCPC mixing and extrusion was less than 2 minutes. The injectability was thereafter calculated as the mass percentage of frCPC that was fully extruded, according to eqn (1). Injectability (%, n = 5) was reported as percentage mean value ± standard deviation.

Injectability:

$$\%I = \frac{M_{\mathrm{i}} - M_{\mathrm{n}}}{M_{\mathrm{i}}} \times 100\%, \tag{1}$$

where M_{n} is the mass of CPC paste that remained in the syringe + cannula after extrusion and M_{i} is the mass of CPC paste before extrusion.

The cohesion of CPCs has been previously defined as the ability to retain its mass in a homogeneous single unit without loss of material due to fragmentation or disintegration upon immersion in an aqueous environment.[23,25] Therefore, to assess the cohesion, frCPCs were injected through the above-mentioned cannula into a phosphate-buffered saline (PBS; Gibco®, Thermo Scientific, Waltham, MA, USA) solution preheated to 37 °C. Immediately after extrusion, cements were qualitatively analyzed to its degree of particulate cloud formation and fragmentation. A score was attributed according to previously reported grading system (Table S1, ESI†). Subsequently, all cements were left soaking in PBS for 24 hours on a shaking plate at 37 °C, after which a new analysis was performed. In order to obtain a final cohesion score that accounts for both the particulate cloud formation and fragmentation,[23] eqn (2) was used.

Cohesion score:

$$C = \frac{\mathrm{PC} + F}{2}, \tag{2}$$

where PC is the particulate cloud formation grade and F is the fragmentation grade.

2.3. Assessment of *in vitro* mechanical properties of frCPC

A Universal Testing Machine (Lloyd Instruments Ltd, Bognor Regis, UK) was used to perform both a uniaxial compression assay and a standard three-point flexural test. In addition to the CPC-based cements, a commercially available poly(methyl methacrylate) (PMMA) spine cement (Vebroplast®, Leader Biomedical BV, Nijmegen, The Netherlands) was also mechanically tested and served as a control.

All cements (n = 10) were prepared by combining the solid and liquid phases and mixing them vigorously for approximately 45 s until homogeneity was reached. Further, samples were extruded through the cannula into molds. For the three-point flexural test rectangular parallelepipedal polydimethylsiloxane (PDMS) molds (25 × 4 × 4 mm) were selected, while cylindrical Teflon molds (6 × 12 mm) were used for the compression test. Following extrusion of the paste, all molds were quickly clamped between two glass slides and allowed to set for 24 h at room temperature. After setting, the specimens were unmolded and carefully inspected for fractures or defects, where sub-optimal specimens were removed from the study. All cements were then immersed in phosphate-buffered saline solution (PBS) and placed on a shaker table set to 120 rpm in an incubator at 37 °C for 72 h to allow the CPC to fully cure. Mechanical testing was performed immediately after removing the cement specimens from the PBS solution in order to ensure testing was performed under wet conditions.

The three-point flexural test was performed by using a method described previously.[26] In brief, each specimen was tested with a pre-load of 1 N, at a cross-head speed of 1 mm s^{-1} and on a support span of 20 mm. The load-displacement curves obtained during this test were further used to calculate the flexural strength (S), flexural modulus (E) and work-of-fracture (WOF), as described in eqn (3)–(5). To allow for a quantitative comparison of WOF values between all experimental groups, the test was automatically terminated when displacement values reached a maximum of 3 mm.

Flexural strength:

$$S = \frac{3FL}{2bl^2}, \tag{3}$$

where F represents the maximum load on the load-displacement curve, L is the support span, and b and l indicate the specimen's width and height, respectively.[30,31]

Flexural modulus:

$$E = \frac{mL^3}{4bl^3}, \tag{4}$$

where m indicates the slope of the line tangent to the linear-elastic portion of the load-displacement curve.[30,31]

Open Access Article. Published on 24 June 2020. Downloaded on 10/19/2025 9:03:45 PM.
This article is licensed under a Creative Commons Attribution 3.0 Unported Licence.

Work-of-fracture:

$$\mathrm{WOF} = \frac{\Omega_u}{bl}, \tag{5}$$

where Ω_u refers to the area under the load-displacement curve.

The compression assay was performed by using a pre-load of 1 N and a cross-head speed of 1 mm s^{-1}. The compression load-displacement curves obtained during this test were further used to calculate the compression strength (σ_ρ) and the compressive work-of-fracture (W_{cu}) as described in eqn (6) and (7). The compressive work-of-fracture (W_{cu}) reflects the capacity of cements to dissipate energy under compression.[26] In order to allow for a consistent calculation of the W_{cu}, all tests were automatically stopped once the specimen reached a compressive strain of 30%.

Compression strength:

$$\sigma_\rho = \frac{F}{A_0}, \tag{6}$$

where A_0 corresponds to the original cross-sectional area of the samples.

Compressive work-of-fracture:

$$W_{cu} = \frac{\Omega_u}{A_0 l} \tag{7}$$

Finally, the compressive modulus (E) was derived from the slope of the linear-elastic portion of the stress–strain curve.

2.4. *Ex vivo* study

***Ex vivo* model, defect creation and cement filling.** The performance of frCPCs and PMMA used in a vertebral augmentation procedures was assessed *ex vivo*, based on previously reported biomechanical *ex vivo* models using CPC-based cements.[5,32] A total of six porcine vertebral bodies were obtained from a slaughterhouse (P.C. van den Berg Vleeshandel Dodewaard, The Netherlands), from which only the lumbar section (*i.e.* L1–L5) was selected for further analysis. Each vertebral body was then carefully detached, cleaned from soft tissue and transverse spinous processes, wrapped in gauze soaked in PBS, and frozen at −20 °C.

A bone defect (5 × 10 mm) was transpediculary drilled though each vertebra in frozen state to minimize the detrimental effect of the heat of the drill on the bone structure. Further, each vertebra was allowed to thaw for exactly 60 minutes at room temperature, after which the cements (CPC, frCPC or PMMA) were retrogradely injected through the cannula into the defect. Vertebrae were then submerged in PBS at 37 °C for 24 hours to allow for setting of the injected cement and rehyradation of the bone structure. All specimens were then removed from PBS, re-wrapped in PBS-soaked gauze, and refrozen at −80 °C.

Assessment of defect filling and cement extravasation. X-rays scans of the injected vertebra were obtained to further analyze the efficiency of the different cements to fill bone defects. X-ray scans were obtained (Planmeca ProX™, Helsinki, Finland) at a standard distance of 10 cm.

In order to compare the extravasation of the different cements into the area surrounding the bone defect, nano-computed tomography was performed on all injected vertebrae. Specimens were scanned using a nano-CT system (GE Phoenix Nanotom M, research edition, General Electric, Wunstorf, Germany) at a voltage of 90 kV and a focal spot size of 2.34 μm. In addition, a longitudinal cross section (~2 mm thick) of the bone defect filled with either frCPC or PMMA and the surrounding bone was prepared by using a diamond saw. The section was freeze-dried and further sputter-coated with a 40 nm thick chromium layer and imaged using a scanning electron microscope (SEM; Zeiss Sigma 300, Zeiss AG, Oberkochen, Germany). Finally, Energy-Dispersive X-ray Spectroscopy (EDX) was performed to distinguish the injected cements (*i.e.* frCPC and PMMA) from the surrounding bone.

Biomechanical compression tests. Cancellous bone cylinders (7 mm diameter and 14 mm height) were prepared from the central part of the frozen vertebral bodies, using a trephine drill parallel to the longitudinal axis of the vertebrae. This direction was selected since it represents the main loading axis in humans.[32] The top and bottom of the cylinders were then flattened by using a rotating sanding station under constant cooling. Special care was taken to ensure size uniformity between specimens, and only cylinders containing a filled bone defect surrounded by bone were kept for further mechanical analysis. All specimens (n = 10) were then again placed in PBS for 24 h, after which they were immediately subjected to a uniaxial, monotonic compression test.

Cylinders were placed in a custom-made chamber containing PBS heated to 37 °C attached to a universal mechanical testing equipment, which allowed to perform the biomechanical tests under physiological conditions. Specimens were subjected to a pre-load of 0.2 N and compressed at a constant speed of 0.1 mm min^{-1}. Compression strength, compression modulus and work of compression were calculated as described above. A consistent calculation of the work of compression was enabled by stopping the compression assay automatically at a standard compressive strain.

2.5. Statistical analysis

All data are presented as a mean ± standard deviation. Statistical analysis was performed using GraphPad Prism® software (version 5.03; GraphPad Software Inc., San Diego, USA) with a level of significance of $p < 0.05$. A one-way analysis of variance (ANOVA) with a *post-hoc* Tukey–Kramer multiple comparisons test was used to analyze quantitative data related to handling and mechanical properties.

3. Results

3.1. Handling properties

Initial setting time values (Fig. 1A) ranged from 2.4 ± 0.2 min to 3.1 ± 0.3 min for all CPCs. For unreinforced CPCs (*i.e.* CPC and CPC/CMC), the addition of CMC caused a significantly increased ($p < 0.05$) initial setting time. With respect to final

 This journal is © The Royal Society of Chemistry 2020

Open Access Article. Published on 24 June 2020. Downloaded on 10/19/2025 9:03:45 PM.
This article is licensed under a Creative Commons Attribution 3.0 Unported Licence.

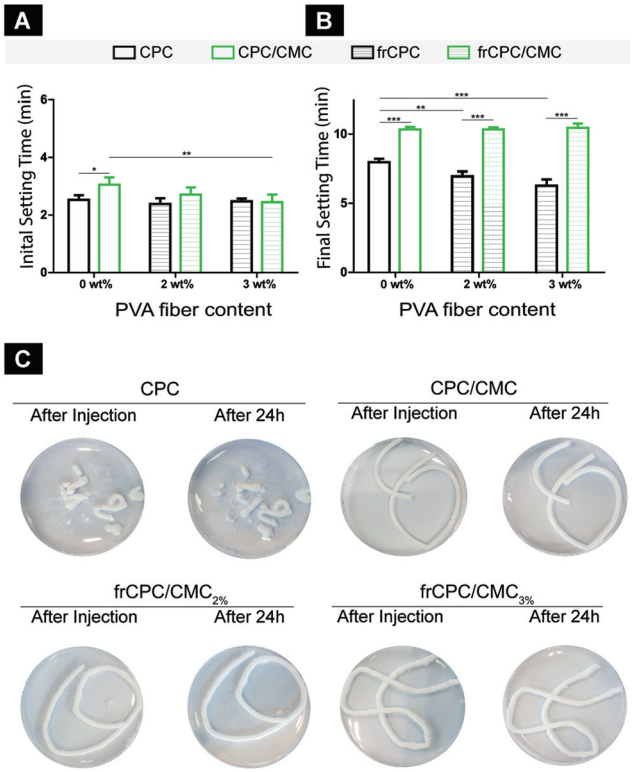

Fig. 1 Handling properties of the different CPC formulations. The initial (A) and final (B) setting times as a function of the quantity (wt%) of PVA fiber for both CPC and CPC/CMC. Statistically significant differences are indicated by $*p < 0.05$, $**p < 0.01$ and $***p < 0.001$. (C) Photographs of extruded cements, immediately and 24 hours after extrusion.

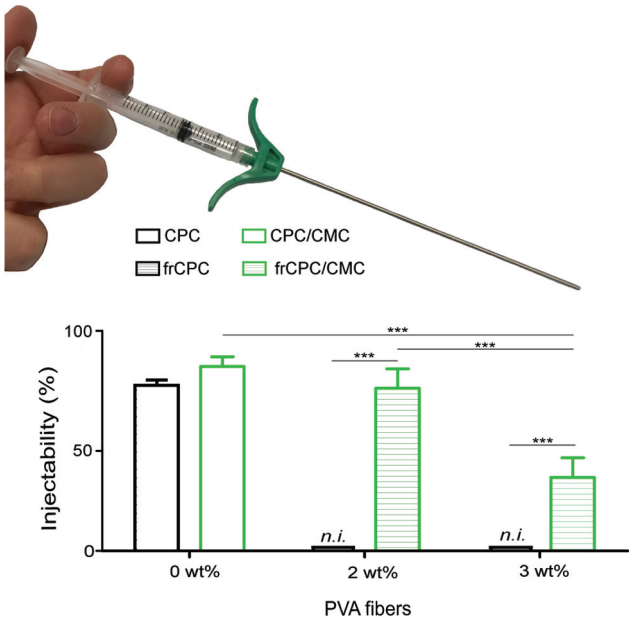

Fig. 2 Injectability (%) of different cement formulations. The photograph shows the syringe + cannula injection device used in this experiment for extrusion of all pastes. The graph illustrates the injectability (%) of the studied formulations as a function of wt% of fiber present in CPC and CPC/CMC. n.i. refers to non-injectable. Statistically significant differences are indicated by $p < 0.001$.

setting times (Fig. 1B), values ranged from 6.8 ± 0.4 min to 10.5 ± 0.3 min. Here, the addition of CMC significantly increased the final setting time of all CPCs as compared to the CMC-free analogues. Additionally, a significantly decreased final setting time was observed for CMC-free CPCs upon addition of PVA fibers.

Cement cohesion was enhanced significantly as a direct consequence of the addition of CMC (Table 2). Cohesion scores showed a clear enhancement from 3.5 ± 0.3 for CMC-free CPC to 1.4 ± 0.3 for CPC/CMC. Visually, CPCs showed virtually no cohesion, while CPC/CMCs allowed for the extrusion of a continuous tube that did neither fragment upon contact with PBS nor disintegrate during setting (Fig. 1C). The addition of PVA fibers did not alter the cohesion of the cement, with CPC/CMC, CPC/CMC$_{2\%}$ and CPC/CMC$_{3\%}$ showing very similar grades of cohesion and visual appearance, both immediately and 24 h after extrusion.

Fig. 2 reveals that injectability ranged from 0% to 92.2 ± 4.8% by extruding the cements through a cannula that is clinically applied for vertebroplasty procedures. The addition of CMC slightly increased injectability values from 82.8 ± 2.7% to 92.2 ± 4.8%. However, for both frCPCs, the addition of CMC rendered these cements injectable (*i.e.* from non-injectable to 81.3 ± 9.7% and 36.7 ± 9.8% for 2 and 3% frCPC/CMC, respectively). Moreover, the quantity of fiber present in the CPC played an important role, as 3 wt% of PVA fiber caused clogging of the syringe and impeded with homogeneous extrusion of the frCPC/CMC paste through the syringe and cannula. Due to non-injectability of frCPCs, these CPCs were not further studied.

3.2. *In vitro* mechanical properties

Fig. 3 shows the flexural properties of PMMA and CPC cements. Stress–strain curves (Fig. 3A) demonstrate that PMMA cements revealed flexural strengths up to ~60 MPa, and failed in a brittle manner at low strain values (~5%). A similar brittle failure behavior was observed for the fiber-free CPCs

Table 2 Cohesion score of different cement formulations

Cohesion score	CPC	frCPC$_{2\%}$	frCPC$_{3\%}$	CPC/CMC	frCPC/CMC$_{2\%}$	frCPC/CMC$_{3\%}$
After injection	3.5 ± 0.3	n.i.	n.i.	1.3 ± 0.2	1.2 ± 0.2	1.2 ± 0.3
After 24 h	4.2 ± 0.3	n.i.	n.i.	1.4 ± 0.3	1.2 ± 0.2	1.2 ± 0.3

n.i.: non-injectable.

Open Access Article. Published on 24 June 2020. Downloaded on 10/19/2025 9:03:45 PM.
This article is licensed under a Creative Commons Attribution 3.0 Unported Licence.

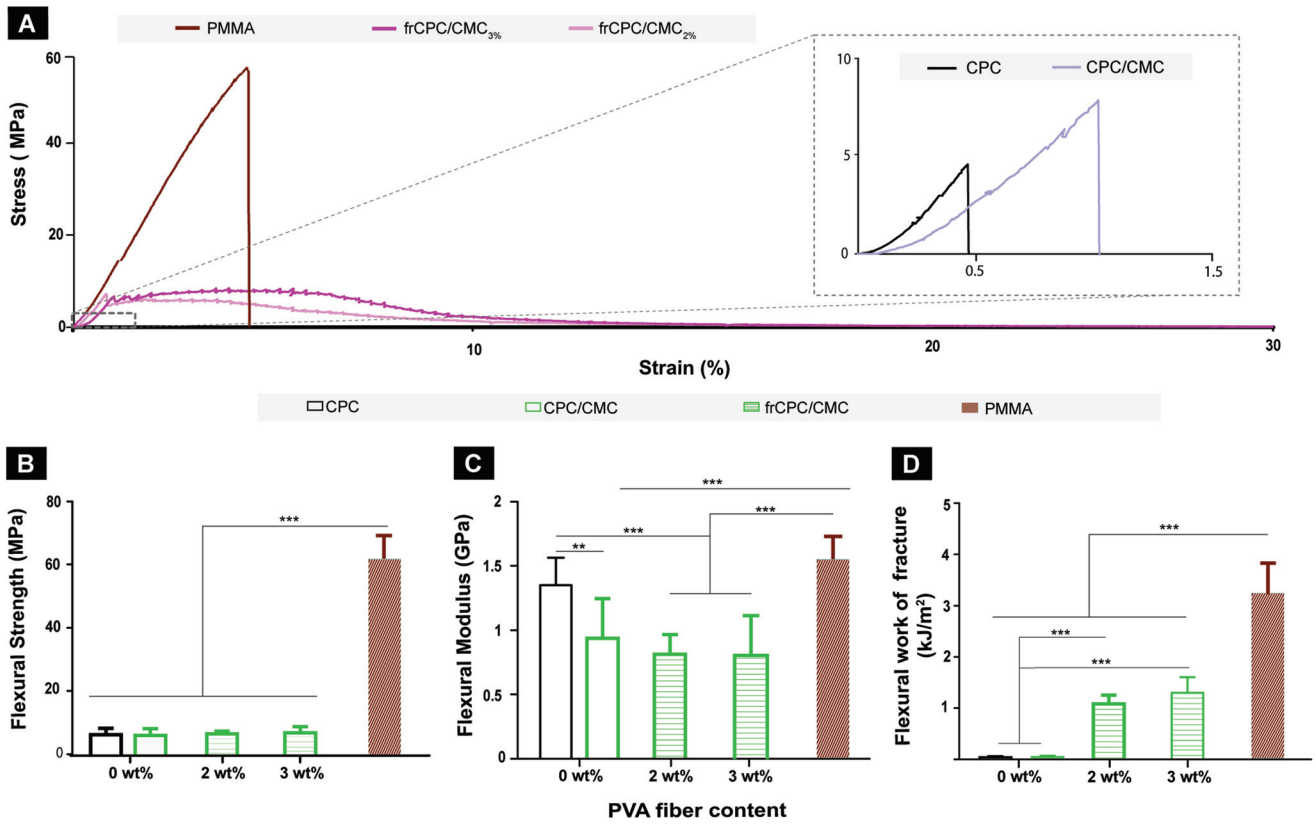

Fig. 3 – Effect of CMC and PVA fiber inclusion on the flexural properties of CPC and PMMA cement. (A) Stress–strain curves, (B) flexural strength, (C) flexural modulus and (D) flexural work of fracture of CPC and PMMA cements. Statistically significant differences are indicated by**$p < 0.01$ and ***$p < 0.001$.

(*i.e.* CPC and CPC/CMC), although CPCs failed at lower stain values (<1.5%) and lower loads than PMMA. Contrarily, both frCPCs (*i.e.* frCPC/$CMC_{2\%}$ and frCPC/$CMC_{3\%}$) exhibited stress–strain curves characteristic of quasi-brittle materials: maximum stress values were reached at relatively low strain values and followed by considerable plastic deformation instead of abrupt rupture. Accordingly, flexural strength of PMMA cement was considerably higher than CPC (Fig. 3B). Further, Fig. 3C shows that the inclusion of CMC significantly decreased the flexural modulus in CPCs, while the incorporation of fibers, irrespective of the amount, hardly affected the flexural modulus.

The flexural work-of-fracture values presented in Fig. 3D clearly show that the presence of PVA-fiber in the CPCs significantly increased their work-of-fracture from ~0.1 ± 0.0 kJ m^{-2} of CPCs to 1.1 ± 0.2 kJ m^{-2} for CPC/$CMC_{2\%}$ and 1.3 ± 0.3 kJ m^{-2} for CPC/$CMC_{3\%}$. Moreover, the increase in fiber percentage from 2 to 3% for frCPC/CMCs did not increase the flexural work-of fracture values. For this reason, and since CPC/$CMC_{3\%}$ exhibited suboptimal injectability of 36.7 ± 9.8% (Fig. 2), the latter group was excluded from further analysis.

The mechanical performance of CPCs and PMMA under compression is presented in Fig. 4. Stress–strain curves (Fig. 4A) show that the compressive strength of PMMA was considerably stronger than CPCs, both before and after reaching the highest compressive stress. Accordingly, PMMA showed significantly ($p < 0.001$) higher compression strength (Fig. 4B) and compressive work-of-fracture (Fig. 4D) than CPC groups, with values being approximately 3- and 5-fold higher for PMMA than for CPC, respectively. In addition, compressive work-of-fracture values (Fig. 4C) for CPC groups were also significantly higher in the presence of PVA (*i.e.* frCPC/$CMC_{2\%}$) compared to fiber-free analogues (*i.e.* CPC and CPC/CMC). Finally, cement stiffness (Fig. 4C) significantly decreased ($p < 0.001$) uponaddition of CMC for CPCs, with a decrease in compressive modulus values from 667 ± 133 MPa to 347 ± 89 MPa for CPC/CMC and 342 ± 112 MPa for frCPC/$CMC_{2\%}$.

3.3. *Ex vivo* model

X-ray scans obtained after defect filling (Fig. 5A) demonstrate that the bone defect was sub-optimally filled by CPC. A clear improvement in defect filling was observed when the defect was filled with cements containing CMC (either CPC/CMC or CPC/$CMC_{2\%}$), indicating that the inclusion of CMC in CPC pastes improved defect filling. Further, PMMA cement completely filled the bone defect and resulted in more pronounced extravasation into the surrounding bone.

The observed differences in extravasation between frCPC/$CMC_{2\%}$ and PMMA were further confirmed by μCT analysis (Fig. 5B and C), where frCPC/$CMC_{2\%}$ remained confined

 This journal is © The Royal Society of Chemistry 2020

Open Access Article. Published on 24 June 2020. Downloaded on 10/19/2025 9:03:45 PM.
This article is licensed under a Creative Commons Attribution 3.0 Unported Licence.

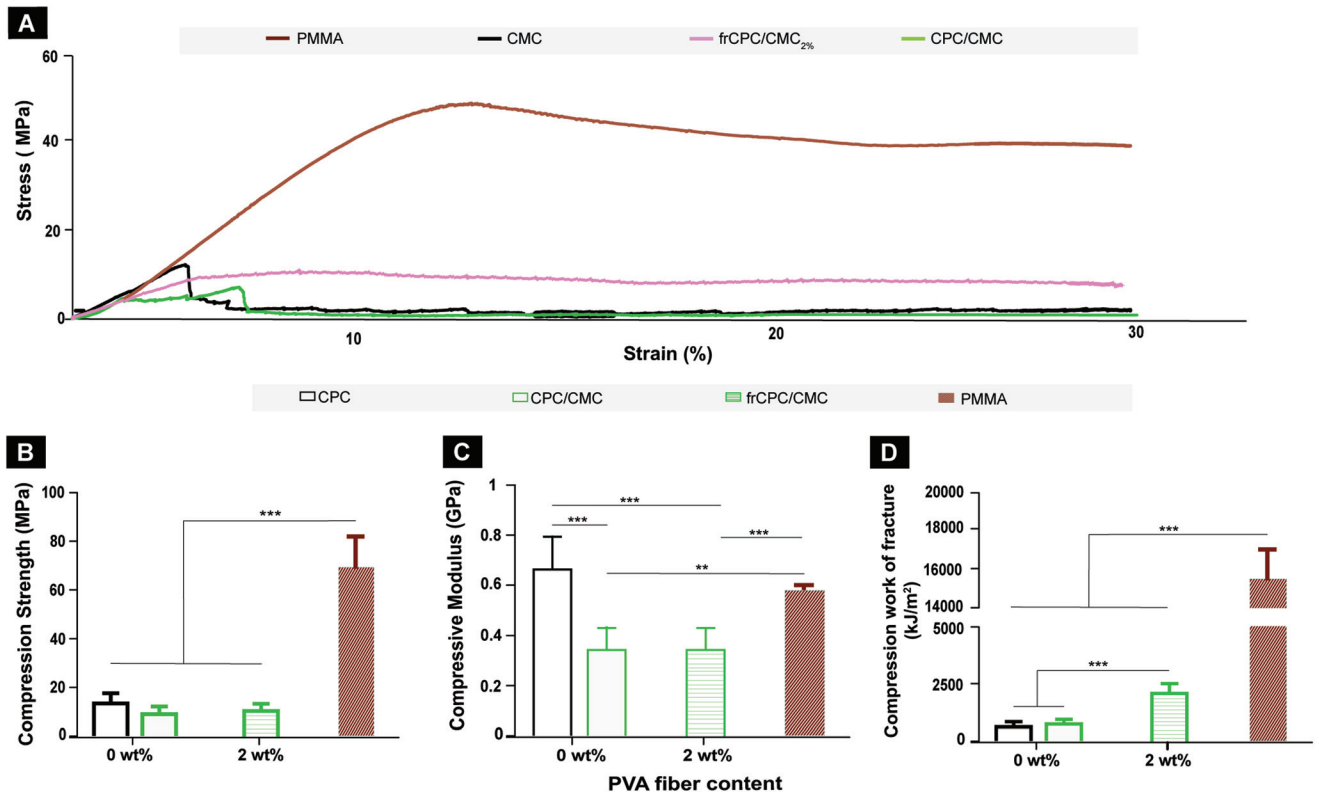

Fig. 4 Effect of CMC and PVA fiber inclusion on the compression properties of CPC formulations and PMMA. (A) Stress–strain curves, (B) compressive strength, (C) compressive modulus and (D) compressive work of fracture. Standard deviations are graphically represented by error bars. Statistically significant differences are indicated by $^{**}p < 0.01$ and $^{***}p < 0.001$.

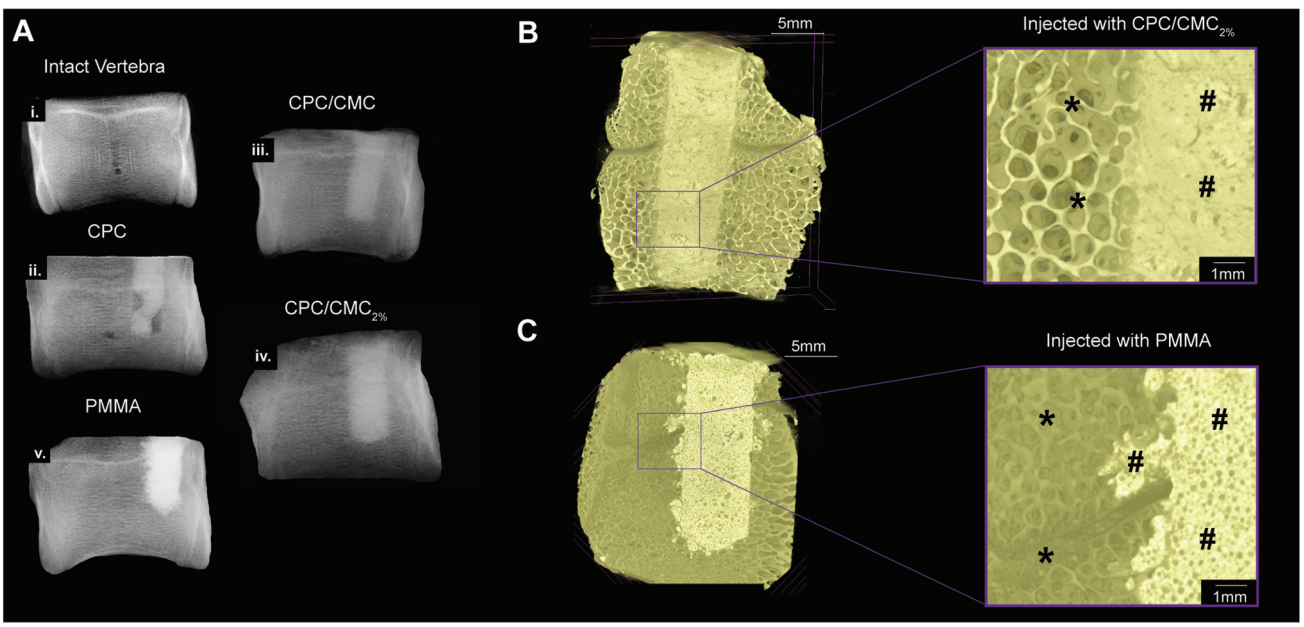

Fig. 5 (A) X-ray scans of porcine vertebrae that were either (i) intact or filled with (ii) CPC, (iii) CMC/CMC, (iv) CPC/CMC$_{2\%}$ and (v) PMMA. μCT images of the bone defects filled with either (B) CPC/CMC$_{2\%}$ or (C) PMMA. * symbols represent bone structure, while # represent bone cement.

Open Access Article. Published on 24 June 2020. Downloaded on 10/19/2025 9:03:45 PM.
This article is licensed under a Creative Commons Attribution 3.0 Unported Licence.

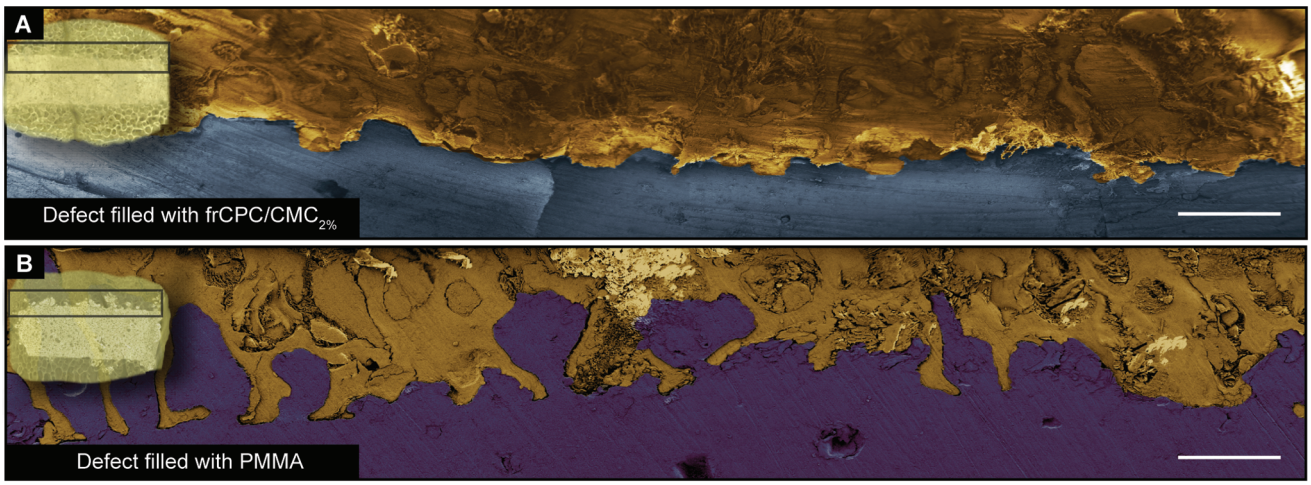

Fig. 6 Scanning electron micrographs of the interface between vertebral bone and cements after filling bone defects with either (A) frCPC/CMC$_{2\%}$ or (B) PMMA. Artificial colorization is used to present frCPC/CMC$_{2\%}$ (dark blue), PMMA (purple) and bone (light brown). Scale bars correspond to 1000 μm.

within the borders of the bone defect, while PMMA cement invaded the pores of adjacent bone tissue. Moreover, scanning electron microscopy (Fig. 6) clearly indicated the difference between bone defect filling patterns for frCPC/CMC$_{2\%}$ and PMMA. While the defect filled with frCPC/CMC$_{2\%}$ (Fig. 6A) remained confined within the limits of the bone defect, PMMA bone cement (Fig. 6B) leached out from the bone defect margins into the porous structure of the sur-

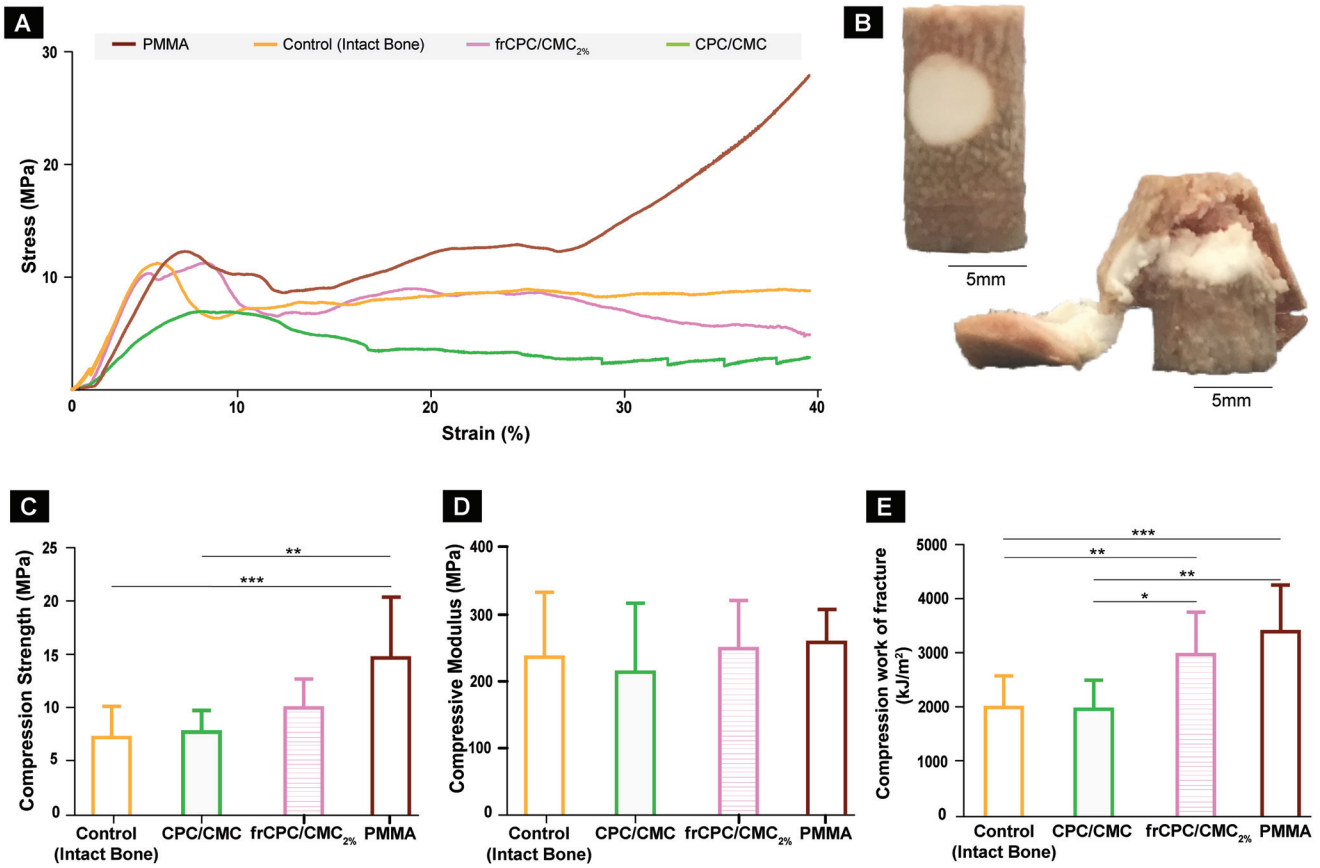

Fig. 7 Biomechanical data obtained from the *ex vivo* assay. (A) Stress–strain curves, (B) representative photographs of the specimens before and after compression assay, (C) compression strength, (D) compressive modulus and (E) compression work of fracture. Statistically significant differences are indicated by *$p < 0.05$, **$p < 0.01$ and ***$p < 0.001$.

 This journal is © The Royal Society of Chemistry 2020

Open Access Article. Published on 24 June 2020. Downloaded on 10/19/2025 9:03:45 PM.
This article is licensed under a Creative Commons Attribution 3.0 Unported Licence.

rounding vertebral cancellous bone, forming extended protrusions.

The stress–strain curves obtained during *ex vivo* biomechanical assessment (Fig. 7A) showed similar linear-elastic behavior for all materials up to the yield point. Consequently, similar compressive moduli were found (range between 215 ± 104 and 258 ± 50; Fig. 7B). After the initiation of plastic deformation, frCPC/$CMC_{2\%}$-treated defects sustained compressive loads similar to intact bone, while PMMA-treated groups supported higher loads with increasing strain. Such mechanical behavior directly impacted compressive strength values, which demonstrated to be superior for PMMA-treated defects (Fig. 7C). Finally, compressive work of fracture values (Fig. 7D) showed that both frCPC/$CMC_{2\%}$ and PMMA rendered the treated vertebrae with significantly higher compressive work-of-fracture values than both intact bone and that the unreinforced groups. No statistical difference was observed for bone samples treated with frCPC/$CMC_{2\%}$ *vs.* PMMA.

4. Discussion

The filling material (*i.e.* bone cement) plays a critical role in the effectiveness of vertebra- and kyphoplasty procedures. In order to achieve long-term sustainability, these bone cements should be osteocompatible and combine adequate mechanical performance with handling properties that facilitate their extrusion *via* minimally invasive surgical procedures.[2] Considering the drawbacks of PMMA cement, a clinical need for an alternative bone cement in vertebra- and kyphoplasty procedures exists. Therefore, extensive research has been dedicated to the development of injectable CPCs. We here aimed to optimize the handling properties of a PVA-fiber reinforced CPC and comparatively studied its biomechanical performance. Our main findings indicate that (i) CMC addition to CPCs improves their handling properties and renders frCPCs injectable without compromising their mechanical properties, (ii) extravasation of frCPC/CMCs to surrounding bone is reduced compared to PMMA, and (iii) *ex vivo* mechanical performance of frCPC/CMC is comparable to PMMA.

The addition of carboxymethyl cellulose (CMC) was previously proven to be an efficient method to render CPC pastes both cohesive and injectable.[23–25,33] In the current study, CMC substantially improved the injectability of frCPCs by acting both as viscosifying and binding agent, hence causing the cement to retain the liquid phase after mixing and improve the distribution of CPC particles within the cement matrix.[33] Consequently, cement flowability increased, the filter-pressing effect[34] was drastically reduced, and injectability was significantly improved. The addition of CMC also contributed to avoid agglomeration of the reinforcing PVA fibers, after the paste was extruded from the cannula (Fig. S1; ESI†).

Injectability studies should, however, be combined with characterization of setting times,[22,34] as several studies[34–37] previously demonstrated that the addition of lubricating agents, while rendering cements injectable, greatly increased their final setting times beyond clinically recommended setting time of 8–15 min for orthopedic applications.[38] In the specific case of CMC, its addition to CPC significantly delayed the (partial) dissolution of calcium phosphate precursor particles during cement hardening, thereby reducing reactivity and increasing final setting times,[24,33] as observed in the current and previous studies.[29,36,39] However, the final setting time of frCPC/CMC as tested in our study remained within the clinical recommendations.

In addition to the incorporation of CMC, the selection of the extrusion device also greatly affects the injectability of frCPCs.[18,34,40] In fact, the commercially available 11G cannula herein used was selected since its internal diameter of 2.39 mm was hypothesized to facilitate the extrusion of the CPC reinforced with 1.5 mm long fibers. We therefore would like to stress that injectability of frCPC as demonstrated herein is highly dependent on the selected experimental conditions. Nonetheless, the currently selected cannula is used in clinics for minimally invasive orthopedic procedures and similar cannulas have been previously reported to successfully deliver CPCs to the spine.[32,40,41] Therefore, by using the here selected cannula, we successfully extruded the frCPC using a protocol that can be easily translated to the clinic.

Once the successful improvement of the handling properties was assessed, we demonstrated that the inclusion of CMC did not affect the mechanical properties of frCPCs.[26] We considered it relevant to evaluate the mechanical properties of frCPC under different load conditions (*i.e.* compression and bending), as both load components are present in the clinical situation. In fact, recent findings in the field of human spine biomechanics caused an update of the classical concept that the spine is almost exclusively subjected to axial compressive loads, to one which also considers shear, bending and torsion load components frequently applied in *e.g.* the lumbar and thoracic section of the spine.[42]

The mechanical properties of frCPC/CMC exceeded those of fiber-free analogues, but were largely inferior to PMMA, when subjected to both bending and compression. According to earlier work, human vertebral trabecular bone has compressive strength values of approximately 5 MPa.[43,44] In this context, the here reported compressive strength of frCPC/CMC (*i.e.* ~18 MPa) demonstrates not only that this material is adequate for vertebral augmentation procedures, but also that its mechanical properties are significantly closer to native bone compared to PMMA.[26,45]

Due to its low initial viscosity, PMMA cements easily invaded the pores of surrounding bone, thereby leading to extra-osseous leakage upon clinical usage.[2,5,46] This leakage was previously reported to cause serious complications such as pulmonary embolism,[47] nerve root compression[48] and even death.[49] Reported solutions to decrease such extra-osseous PMMA leakage mainly rely on increasing cement viscosity prior to injection.[46,50] While some clinical reports show that high-viscosity PMMA cement indeed reduces extra-osseous leakage,[51] others argue that these viscous PMMA cements can hardly be considered injectable (*i.e.* forces required to extrude

Open Access Article. Published on 24 June 2020. Downloaded on 10/19/2025 9:03:45 PM.
This article is licensed under a Creative Commons Attribution 3.0 Unported Licence.

these PMMA cements exceed the human physical limit and require special injecting equipment).[46] In our study, CMC acted as a viscosifying agent for frCPCs, which offered an optimal balance between viscosity, injectability, cohesion and defect filling uniformity. In fact, the viscosity of frCPC/CMC allowed for cement extrusion through the cannula, thereby uniformly filling the bone defect while remaining confined within the limits of the bone defect without leaking into the peripheral bone. Conversely, PMMA leaked out into the surrounding bone, forming structures previously referred to as "fingers of a glove", which spread out fast and are difficult to predict and control.[46,50]

Regarding the *ex vivo* biomechanical assessment, we choose to use a pre-drilled defect for subsequent cement filling rather than artificially creating a vertebral compression fracture, as previously reported.[5,52,53] Three reasons formed the bais for our choice. Firstly, the creation of a defect allowed for a straightforward, reproducible and standardized way of decreasing possible experimental errors that could arise from shape/fracture discrepancy between specimens. Secondly, the selected methodology allowed the *ex vivo* specimens to be manipulated as minimally as possible before their biomechanical evaluation, which avoided excessive drying of the specimens and decreased potential alterations of the mechanical properties of bone.[54] Finally, since this assay aimed to provide *ex vivo* proof-of-concept for the suitability of frCPC for vertebral augmentation, the selected methods should be easily translatable to a subsequent *in vivo* study to confirm the herein obtained results. As reported previously, the direct injection of augmentation cement into fractured or osteoporotic vertebrae (in *e.g.* sheep preclinical models) causes severe complications, such as significant decreases of heart rate and arterial pressure, an increase of the venous pressure, the appearance of showers of echogenic material in the pulmonary artery, and transient changes of blood pH and pCO_2.[55–57] For this reason, recently performed *in vivo* studies,[32,41,50] choose to utilize a low-pressure injecting method through pre-drilled channels that decreases risks and also show high analogy with the cement injection in humans following a pre-formed intravertebral space by balloon expansion during kyphoplasty.

In the *ex vivo* set-up, frCPC/CMC and PMMA showed higher compression strength and compressive work-of-fracture than the remaining groups, while stiffness remained equal for all groups. Interestingly, however, while the compressive strength of the cement-filled vertebrae could only be improved with PMMA, the work-of-fracture values of cement-filled vertebrae was improved both by PMMA and frCPC/CMC. This enhancement indicates that fiber-reinforcement of CPCs improved the work-of-fracture values of cement filled bone to the same level as PMMA-filled vertebrae.

Concerning the chosen biomechanical experimental set-up, all experimental cylindric bone specimens collapsed according to the failure patterns illustrated in Fig. 7B (*i.e.* failure occurred throughout the defect region). This failure pattern seems to indicate that the defect was therefore the most susceptible region of the specimen for mechanical failure. However, all experimental cements, including the non-reinforced CPC/CMC, seemed to confer a reinforcing effect to the vertebrae, as no experimental group performed significantly worse than the intact bone. Consequently, these observations suggest that the bone seems to dominate the mechanical behavior of the tested samples. In other words, while this experimental set-up allowed for a simple assessment of the mechanical behavior of cements injected into bone defects, the size of the defects seems to not have sufficiently weaken the bone structure. Mechanical data from an additional experimental group containing bone specimens with an unfilled defect would potentially allow to clarify this aspect further. However, due to technical limitations, these specimens could not be reliably produced, forcing their exclusion from the study.

5. Conclusions

Herein we have shown that PVA-fiber reinforced CPCs (i) can be rendered injectable, (ii) clinically applicable, and (iii) biomechanically reliable for *ex vivo* vertebral augmentation procedures by inclusion of CMC in the CPC formulation. Comparative *ex vivo* analysis further demonstrated reduced extravasation of frCPC/CMC into the inter-trabecular space and similar biomechanical properties compared to PMMA. Consequently, we conclude that frCPC/CMC cements hold strong promise as spinal bone cement.

Conflicts of interest

There are no conflicts to declare.

Acknowledgements

This work was financially supported by the Netherlands Organization for Scientific Research (NWO; VIDI grant #13455). The authors would like to thank colleagues Natasja van Dijk, Martijn Martens and Vincent Cuijpers for technical assistance.

References

1 U. Nations, *World Population Prospects 2019: Highlights ST/ESA/SER.A*, New York, USA, 2019.
2 Z. He, Q. Zhai, M. Hu, C. Cao, J. Wang, H. Yang and B. Li, *J. Orthop. Transl.*, 2015, **3**, 1–11.
3 M. J. Kim, D. P. Lindsey, M. Hannibal and T. F. Alamin, *Spine*, 2006, **31**, 2079–2084.
4 G. Marcucci and M. L. Brandi, *Clin. Cases Miner. Bone Metab.*, 2010, **7**, 51–60.
5 Q. Lu, C. Liu, D. Wang, H. Liu, H. Yang and L. Yang, *Spine J.*, 2019, **19**, 1871–1884.

 This journal is © The Royal Society of Chemistry 2020

Open Access Article. Published on 24 June 2020. Downloaded on 10/19/2025 9:03:45 PM.
This article is licensed under a Creative Commons Attribution 3.0 Unported Licence.

6 R. S. Taylor, R. J. Taylor and P. Fritzell, *Spine*, 2006, **31**, 2747–2755.
7 R. S. Zhu, S. L. Kan, G. Z. Ning, L. X. Chen, Z. G. Cao, Z. H. Jiang, X. L. Zhang and W. Hu, *Osteoporosis Int.*, 2019, **30**, 287–298.
8 P. Galibert, H. Deramond, P. Rosat and D. Le Gars, *Neurochirurgie*, 1987, **33**, 166–168.
9 A. Boger, P. Heini, M. Windolf and E. Schneider, *Eur. Spine J.*, 2007, **16**, 2118–2125.
10 P. A. Hulme, J. Krebs, S. J. Ferguson and U. Berlemann, *Spine*, 2006, **31**, 1983–2001.
11 Y. Zhan, J. Jiang, H. Liao, H. Tan and K. Yang, *World Neurosurg.*, 2017, **101**, 633–642.
12 I. A. Grafe, M. Baier, G. Noldge, C. Weiss, K. Da Fonseca, J. Hillmeier, M. Libicher, G. Rudofsky, C. Metzner, P. Nawroth, P. J. Meeder and C. Kasperk, *Spine*, 2008, **33**, 1284–1290.
13 D. Lin, J. Hao, L. Li, L. Wang, H. Zhang, W. Zou and K. Lian, *Clin. Spine Surg.*, 2017, **30**, E270–E275.
14 G. H. Xiang, M. J. Tong, C. Lou, S. P. Zhu, W. J. Guo and C. R. Ke, *Pain Physician*, 2018, **21**, 209–218.
15 M. Libicher, J. Hillmeier, U. Liegibel, U. Sommer, W. Pyerin, M. Vetter, H. P. Meinzer, I. Grafe, P. Meeder, G. Noldge, P. Nawroth and C. Kasperk, *Osteoporosis Int.*, 2006, **17**, 1208–1215.
16 J. Zhang, W. Liu, V. Schnitzler, F. Tancret and J.-M. Bouler, *Acta Biomater.*, 2014, **10**, 1035–1049.
17 C. Canal and M. P. Ginebra, *J. Mech. Behav. Biomed. Mater.*, 2011, **4**, 1658–1671.
18 S. V. Dorozhkin, *J. Mater. Sci.*, 2008, **43**, 3028–3057.
19 R. Kruger and J. Groll, *Biomaterials*, 2012, **33**, 5887–5900.
20 T. R. Blattert, L. Jestaedt and A. Weckbach, *Spine*, 2009, **34**, 108–114.
21 I. Khairoun, F. C. Driessens, M. G. Boltong, J. A. Planell and R. Wenz, *Biomaterials*, 1999, **20**, 393–398.
22 M. Bohner, *Eur. Cells Mater.*, 2010, **20**, 1–12.
23 N. W. Kucko, W. Li, M. A. García Martinez, I. U. Rehman, A.-S. T. Ulset, B. E. Christensen, S. C. G. Leeuwenburgh and R.-P. Herber, *J. Biomed. Mater. Res., Part B*, 2019, **107**, 2216–2228.
24 E. C. Grosfeld, J. W. Hoekstra, R. P. Herber, D. J. Ulrich, J. A. Jansen and J. J. van den Beucken, *Biomed. Mater.*, 2016, **12**, 015009.
25 J. An, H. Liao, N. W. Kucko, R. P. Herber, J. G. Wolke, J. J. van den Beucken, J. A. Jansen and S. C. Leeuwenburgh, *J. Biomed. Mater. Res., Part A*, 2016, **104**, 1072–1081.
26 N. W. Kucko, S. de Lacerda Schickert, T. Sobral Marques, R.-P. Herber, J. J. J. P. van den Beuken, Y. Zuo and S. C. G. Leeuwenburgh, *ACS Biomater. Sci. Eng.*, 2019, **5**, 2491–2505.
27 S. de Lacerda Schickert, J. A. Jansen, E. M. Bronkhorst, J. J. J. P. van den Beucken and S. C. G. Leeuwenburgh, *Acta Biomater.*, 2020, **110**, 280–288.
28 N. W. Kucko, D.-G. Petre, M. de Ruiter, R.-P. Herber and S. C. G. Leeuwenburgh, *J. Mech. Behav. Biomed. Mater.*, 2020, **109**, 103776.
29 I. Khairoun, M. G. Boltong, F. C. M. Driessens and J. A. Planell, *J. Mater. Sci. Mater. Med.*, 1998, **9**, 425–428.
30 Y. Zuo, F. Yang, J. G. Wolke, Y. Li and J. A. Jansen, *Acta Biomater.*, 2010, **6**, 1238–1247.
31 V. C. Li, D. K. Mishra and H.-C. Wu, *Mater. Struct.*, 1995, **28**, 586–595.
32 F. Gunnella, E. Kunisch, S. Maenz, V. Horbert, L. Xin, J. Mika, J. Borowski, S. Bischoff, H. Schubert, A. Sachse, B. Illerhaus, J. Gunster, J. Bossert, K. D. Jandt, F. Ploger, R. W. Kinne, O. Brinkmann and M. Bungartz, *Spine J.*, 2018, **18**, 357–369.
33 H. L. R. Alves, L. A. dos Santos and C. P. Bergmann, *J. Mater. Sci. Mater. Med.*, 2008, **19**, 2241–2246.
34 M. Bohner and G. Baroud, *Biomaterials*, 2005, **26**, 1553–1563.
35 J. E. Barralet, L. M. Grover and U. Gbureck, *Biomaterials*, 2004, **25**, 2197–2203.
36 U. Gbureck, J. E. Barralet, K. Spatz, L. M. Grover and R. Thull, *Biomaterials*, 2004, **25**, 2187–2195.
37 L. Leroux, Z. Hatim, M. Frèche and J. L. Lacout, *Bone*, 1999, **25**, 31S–34S.
38 I. Khairoun, M. G. Boltong, F. C. M. Driessens and J. A. Planell, *J. Biomed. Mater. Res.*, 1997, **38**, 356–360.
39 S. Sarda, E. Fernandez, M. Nilsson, M. Balcells and J. A. Planell, *J. Biomed. Mater. Res.*, 2002, **61**, 653–659.
40 E. F. Burguera, H. H. K. Xu and L. Sun, *J. Biomed. Mater. Res., Part B*, 2008, **84**, 493–502.
41 M. Bungartz, S. Maenz, E. Kunisch, V. Horbert, L. Xin, F. Gunnella, J. Mika, J. Borowski, S. Bischoff, H. Schubert, A. Sachse, B. Illerhaus, J. Günster, J. Bossert, K. D. Jandt, R. W. Kinne and O. Brinkmann, *Spine J.*, 2016, **16**, 1263–1275.
42 T. R. Oxland, *J. Biomech.*, 2016, **49**, 817–832.
43 D. P. Fyhrie and M. B. Schaffler, *Bone*, 1994, **15**, 105–109.
44 D. P. Fyhrie and D. Vashishth, *Bone*, 2000, **26**, 169–173.
45 Q. Fu, E. Saiz, M. N. Rahaman and A. P. Tomsia, *Mater. Sci. Eng., C*, 2011, **31**, 1245–1256.
46 G. Baroud, M. Crookshank and M. Bohner, *Spine*, 2006, **31**, 2562–2568.
47 T. Chong, J. Lieu, T. Alamin and R. Mitra, *Pain Pract.*, 2011, **11**, 570–573.
48 D. S. Kim, S. Y. Jang, M. H. Kong, K. Y. Song and D. S. Kang, *Korean J. Neurotrauma*, 2014, **10**, 155–158.
49 H. L. Chen, C. S. Wong, S. T. Ho, F. L. Chang, C. H. Hsu and C. T. Wu, *Anesth. Analg.*, 2002, **95**, 1060–1062, table of contents.
50 L. Xin, M. Bungartz, S. Maenz, V. Horbert, M. Hennig, B. Illerhaus, J. Günster, J. Bossert, S. Bischoff, J. Borowski, H. Schubert, K. D. Jandt, E. Kunisch, R. W. Kinne and O. Brinkmann, *Spine J.*, 2016, **16**, 1468–1477.
51 C. G. Trumm, T. F. Jakobs, R. Stahl, T. A. Sandner, P. M. Paprottka, M. F. Reiser, C. J. Zech and R. T. Hoffmann, *Skeletal Radiol.*, 2013, **42**, 113–120.
52 Z. Zheng, K. D. Luk, G. Kuang, Z. Li, J. Lin, W. M. Lam, K. M. Cheung and W. W. Lu, *Spine*, 2007, **32**, 2076–2082.

53 A. Perry, A. Mahar, J. Massie, N. Arrieta, S. Garfin and C. Kim, *Spine J.*, 2005, **5**, 489–493.
54 J. D. Currey, *J. Biomech.*, 1988, **21**, 439–441.
55 N. Aebli, J. Krebs, D. Schwenke, G. Davis and J. C. Theis, *Spine*, 2003, **28**, 1513–1519.
56 N. Aebli, J. Krebs, D. Schwenke, G. Davis and J. C. Theis, *Spine*, 2003, **28**, 1504–1511.
57 J. Krebs, N. Aebli, B. G. Goss, S. Sugiyama, T. Bardyn, I. Boecken, P. J. Leamy and S. J. Ferguson, *J. Biomed. Mater. Res., Part B*, 2007, **82**, 526–532.

Open Access Article. Published on 24 June 2020. Downloaded on 10/19/2025 9:03:45 PM.
This article is licensed under a Creative Commons Attribution 3.0 Unported Licence.

 This journal is © The Royal Society of Chemistry 2020